Applied Geochemistry 50 (2014) 91–105

Contents lists available at ScienceDirect

Applied Geochemistry

journal homepage: www.elsevier.com/locate/apgeochem

Rock alteration in alkaline cement waters over 15 years and its relevance to the geological disposal of nuclear waste

Elizabeth B.A. Moyce [a], Christopher Rochelle [c], Katherine Morris [b], Antoni E. Milodowski [c], Xiaohui Chen [d], Steve Thornton [d], Joe S. Small [e], Samuel Shaw [b,*]

[a] Earth Surface Science Institute, School of Earth and Environment, University of Leeds, Leeds LS2 9JT, UK
[b] Research Centre for Radwaste Disposal, School of Earth, Atmospheric and Environmental Sciences, The University of Manchester, Manchester M13 9PL, UK
[c] British Geological Survey, Nicker Hill, Keyworth, Nottingham NG12 5GG, UK
[d] Kroto Research Institute, University of Sheffield, Sheffield S10 2TN, UK
[e] National Nuclear Laboratory, Birchwood Park, Warrington WA3 6AE, UK

ARTICLE INFO

Article history:
Available online 7 September 2014
Editorial handling by M. Kersten

ABSTRACT

The interaction of groundwater with cement in a geological disposal facility (GDF) for intermediate level radioactive waste will produce a high pH leachate plume. Such a plume may alter the physical and chemical properties of the GDF host rock. However, the geochemical and mineralogical processes which may occur in such systems over timescales relevant for geological disposal remain unclear. This study has extended the timescale for laboratory experiments and shown that, after 15 years two distinct phases of reaction may occur during alteration of a dolomite-rich rock at high pH. In these experiments the dissolution of primary silicate minerals and the formation of secondary calcium silicate hydrate (C–S–H) phases containing varying amounts of aluminium and potassium (C–(A)–(K)–S–H) during the early stages of reaction (up to 15 months) have been superseded as the systems have evolved. After 15 years significant dedolomitisation ($MgCa(CO_3)_2 + 2OH^- \rightarrow Mg(OH)_2 + CaCO_3 + CO^{2-}_{3(aq)}$) has led to the formation of magnesium silicates, such as saponite and talc, containing variable amounts of aluminium and potassium (Mg–(Al)–(K)–silicates), and calcite at the expense of the early-formed C–(A)–(K)–S–H phases. This occurred in high pH solutions representative of two different periods of cement leachate evolution with little difference in the alteration processes in either a KOH and NaOH or a $Ca(OH)_2$ dominated solution but a greater extent of alteration in the higher pH KOH/NaOH leachate. The high pH alteration of the rock over 15 years also increased the rock's sorption capacity for U(VI). The results of this study provide a detailed insight into the longer term reactions occurring during the interaction of cement leachate and dolomite-rich rock in the geosphere. These processes have the potential to impact on radionuclide transport from a geodisposal facility and are therefore important in underpinning any safety case for geological disposal.

1. Introduction

A widely recognised concept for the disposal of radioactive waste, which will remain hazardous for hundreds of thousands of years, is emplacement in a geological disposal facility (GDF). Many proposed GDF concepts for Intermediate Level Waste (ILW), such as those in the UK, France, Canada and Switzerland (NDA, 2010a; Andra, 2012; Nuclear Waste Management Organisation, 2010; Nagra, 2014), involve cement e.g. as a waste-form, backfill and construction material. Post-closure, groundwater will saturate the facilities and cement dissolution will produce a high pH leachate which will evolve in composition and pH over the lifetime of the GDF (Atkinson, 1985; Berner, 1992). Initially, dissolution of KOH and NaOH within the cement will form a leachate of pH ~13. The leachate pH will then decrease to ~12.5 where it will be buffered by equilibration with portlandite ($Ca(OH)_2$). The leachate will remain at this pH until all the $Ca(OH)_2$ has dissolved, after which, pH will be controlled by equilibrium with calcium silicate hydrate (C–S–H) gel and will decrease to ~10.5. The leachate will form a chemically disturbed zone (CDZ) in the geosphere surrounding the GDF, also known as an alkaline disturbed zone (ADZ; NDA, 2010b). Previous studies have shown that in the CDZ high pH leachates could cause the dissolution of aluminosilicate minerals and formation of secondary mineral phases (e.g. C–S–H phases, Gaucher and Blanc, 2006 and references therein)). This could

* Corresponding author.
E-mail address: sam.shaw@manchester.ac.uk (S. Shaw).

http://dx.doi.org/10.1016/j.apgeochem.2014.08.003
0883-2927/

change the physical (e.g. porosity and permeability) and chemical (e.g. reactive surface area and sorption capacity) properties of the host rock thereby affecting radionuclide transport. For example, mineral dissolution could increase rock permeability and promote radionuclide transport, or the formation of secondary solid phases could block flow paths and have the opposite effect. The formation of secondary phases will also change the nature of the surfaces with which radionuclides could interact e.g. any increased sorption capacity of secondary phases could retard contaminant transport. The potential for cement leachates to alter host rock properties shows that understanding the chemical and mineralogical changes which occur will be key to developing a long term safety case for any cementitious GDF. However, there is a lack of long-term (>10 years) experimental studies which investigate these processes.

Overall, is has been suggested that CDZ alteration can be divided into two regions (Savage, 2011). Firstly, a zone closest to the cement/rock interface (zone 1) where extensive mineral alteration occurs, including dissolution of primary silicate minerals and precipitation of secondary solid phases. Secondly, a zone further from the interface (zone 2) where fluid chemistry is perturbed and ion exchange reactions are important, but rock alteration is significantly diminished. Many short term laboratory and underground rock laboratory experimental studies have investigated rock and mineral alteration in high pH cement leachates (zone 1; e.g. Gaucher and Blanc, 2006; Bateman et al., 1999; and references therein; Braney et al., 1993; Cuevas, 2004; Mäder et al., 2006). Generally, these studies have found that reaction in high pH, Ca-bearing cement-type leachates results in the dissolution of silicate minerals (Eq. (1)) followed predominantly by the precipitation of secondary C–S–H phases (Eq. (2)) of varying Ca:Si ratio (e.g. 0.5–1.5 (Gaucher and Blanc, 2006)), morphology and crystallinity e.g. C–S–H gel (Savage and Rochelle, 1993; Hodgkinson and Hughes, 1999).

$$KAlSi_3O_8 + 3OH^- + 2H_2O \rightarrow Al(OH)_4^- + 3HSiO_{3(aq)}^- + K_{(aq)}^+ \quad (1)$$

$$HSiO_{3(aq)}^- + Ca_{(aq)}^{2+} + H_2O \rightarrow C-S-H_{gel} \quad (2)$$

where aluminium (e.g., from primary mineral dissolution) and potassium (e.g. dissolved in cement leachate) are present, secondary aluminium and potassium bearing C–S–H (C–(A)–(K)–S–H) phases have also been identified (e.g. Braney et al., 1993; Savage et al., 1992). Studies of clay alteration (e.g. bentonite) at high pH found the formation of a number of Na/K/Ca bearing silicate phases including zeolites (e.g. phillipsite $(K,Na,Ca)_{1-2}(Si,Al)_8O_{16}\cdot 6H_2O$, analcime $NaAlSi_2O_6\cdot H_2O$) and apophyllite ($KCa_4Si_8O_{20}(OH)\cdot 8H_2O$) (Gaucher and Blanc, 2006; Ramirez, 2005). Carbonate may also be released into solution during high pH rock alteration. For example, cement pore water can promote the breakdown of dolomite ($CaMg(CO_3)_2$) according to the reaction shown in Eq. (3) (Poole and Sotiropoulos, 1980; Bérubé et al., 1990; Braithwaite and Heath, 2013 and references therein) releasing carbonate to solution leading to the formation of calcium carbonate minerals e.g. calcite. However, these processes have not been studied in the context of the CDZ.

$$MgCa(CO_3)_2 + 2OH^- \rightarrow Mg(OH)_2 + CaCO_3 + CO_{3(aq)}^{2-} \quad (3)$$

Generally, experimental studies have limited timescales, with few longer than 1–2 years (e.g. a 540 day experiment is the longest study reviewed by Gaucher and Blanc, 2006) and no longer-term experimental studies examine the stability of the secondary phases formed. However, GDFs will evolve over tens to hundreds of thousands of years. To investigate the effect of high pH alteration at timescales more comparable to GDF scenarios, natural and anthropogenic analogue sites have been studied. At natural analogue sites such as Maqarin, Jordan (Milodowski et al., 1998; Alexander, 1992; Alexander et al., 2012; Linklater, 1998; Savage, 2011) and Troodos, Cyprus (Alexander et al., 2011), alkaline groundwaters have interacted with rock at timescales extending beyond 1 million years. Whereas anthropogenic analogue sites (e.g. the Tournemire Tunnel; Tinseau et al., 2006; Techer et al., 2012) bridge the gap between laboratory experiments and natural analogues. A review of many such sites representing timescales of alteration from ~30 years to >1 million years is provided by Savage (2011). Overall, these studies indicate that over time a variety of secondary phases can form, predominantly alkali-silica gels (e.g. C–S–H gel), which can crystallise with time to zeolites, C–S–H minerals e.g. okenite ($CaSi_2O_5\cdot 2H_2O$), and feldspars. The key factors controlling which phases form are primarily solution composition (e.g. pH) and reaction time. Modelling has also been used to predict the chemical and physical evolution within the CDZ (e.g. Savage et al., 1992; Savage and Rochelle, 1993; Braney et al., 1993; Bateman et al., 1999; Pfingsten et al., 2006; Soler and Mäder, 2007; Fernandez et al., 2010; Alexander et al., 1992). These studies generally support the experimental findings that silicate mineral dissolution is followed by secondary solid phase (e.g. C–S–H) formation, with subsequent transformation of C–S–H to feldspar and zeolite over time, as found at analogue sites. However, modelling predictions are limited by the ability to constrain which solids will form due to slow reaction rates, and a lack of reliable thermodynamic data for some phases (e.g. C–S–H gel).

The secondary solid phases produced during high pH rock alteration may affect radionuclide migration through the CDZ by changing the sorption properties of the material. A key radionuclide of concern is U(VI) which is highly mobile and hazardous over the long timescales relevant to geological disposal (NDA, 2010c). As C–S–H has been found to be the predominant secondary phase produced by high pH rock alteration and is also the most abundant phase in hardened cement paste (Taylor, 1990), which is used as an ILW wasteform, the interaction of U(VI) with these phases has been studied in some detail (Harfouche et al., 2006; Tits et al., 2011; Gaona et al., 2012; Atkins and Glasser, 1992). However, few experimental studies have looked at the interaction of U(VI) with secondary phases in-situ following high pH mineral/rock alteration and these have generally been limited to investigation after only several months of high pH reaction (e.g. Berry et al., 1999). Continued evolution of altered material over decades may further change surface properties and so affect U(VI) interactions. Therefore experimental investigation of these interactions with rock after extended periods of alteration could help fill this knowledge gap.

1.1. Review of alteration experiment up to 15 months

In this study rock alteration by high pH cement waters has been characterised in unique experiments lasting over 15 years, providing new insight into longer-term rock alteration. These experiments were originally part of the Nirex Safety Assessment Research Programme (NSARP) run by the British Geological Survey (BGS). The experiments were started in 1995 and the rock type and solution compositions used reflect the focus of NSARP at that time (Rochelle et al., 1997; details of how to access this report are provided in Supporting Information). However, as the rock contains many common rock-forming minerals the long-term alteration processes which have occurred will be representative of many rock types. The experiments investigate reaction of disaggregated dolomite-rich fracture fill rock (Borrowdale Volcanic Group (BVG), UK) with fluids representative of young (pH 13, Young Near Field Pore-water (YNFP) and intermediate (pH 12, Evolved Near Field Groundwater (ENFG)) cement leachates. The products of these experiments (fluid and solid phases) were initially investigated up to 15 months of reaction, and a full description of the results

up to that point is presented elsewhere (Rochelle et al., 1997). However, a brief summary of the results is given here. Characterisation of the rock surfaces indicated intensive dissolution of primary silicate minerals (e.g. feldspar), and the formation of poorly crystalline alkali silicate gels (i.e. C–(A)–(K)–S–H phases), and less abundant crystalline apophyllite–KOH. Although the solid secondary phases produced in both leachates were similar, alteration was more extensive in the pH 13 YNFP system. Analysis of the pore fluids showed that the pH of the YNFP and ENFG reduced to 11.8 and 9.7 respectively. During this time the concentration of dissolved Si and Al increased significantly, due to the dissolution of the silicate minerals, and the Ca concentration decreased due to the precipitation of Ca-rich secondary phases. Overall, the reaction followed the 2-stage dissolution and precipitation process observed in other studies. However, the data indicated that the system was not at equilibrium (i.e. the concentration of ions in solution was not stable) and that further evolution of the system may occur over a longer timescale. For example, the dolomite in the rock may undergo dedolomitisation (Eq. (3)) as observed by (Bérubé et al., 1990), leading to the release of significant amounts of carbonate and magnesium.

The aim of this study was to characterise the evolution of the BVG alteration experiments after 15 years of reaction and determine the influence of rock alteration on its reaction with U(VI). This was achieved through (1) characterisation of the changes in fluid composition and solid phase stability, crystallinity and composition between 15 months and 15 years of reaction; (2) assessment of any difference in reactions due to leachate composition; (3) comparison of U(VI) interactions with unaltered rock and rock altered at high pH for 15 years. This work will aid understanding of the longer term effects of the cement leachate on rock alteration and radionuclide transport in the CDZ.

2. Materials and methodology

A full description of the experimental method is provided by Rochelle et al. (1997). A summary is given here. The rock used in the experiments was altered wallrock and dolomite-mineralised fracture fill from a hydrogeologically conductive fracture zone in the BVG, Ordovician basement volcanic rocks, UK (Milodowski et al., 1998). It was collected from the United Kingdom Nirex borehole BH14A in Cumbria, UK at 859 m depth (UK grid reference NY 0248 0569) (Rochelle et al., 1997, see Supporting Information for access details). A large (1–2 kg) sample of the rock was disaggregated and sieved. A sub-sample of the 125–250 μm size fraction was then reacted with two synthetic cement leachates. The leachates were designed (see Table 1) to represent a young near field pore water (YNFP; pH 13.0 at 25 °C) and an evolved near field groundwater (ENFG; pH 12.2 at 25 °C). The YNFP was dominated by dissolved KOH and NaOH, and saturated with respect to $Ca(OH)_2$, and the ENFG represented a synthetic deep groundwater (i.e. high salinity, Na/CaCl and $NaSO_4$ rich), saturated with respect to $Ca(OH)_2$. The ENFG included the influence of deep groundwater, but the YNFP does not because a significant amount of time would be required for groundwater to ingress into the repository. Each solution was prepared under a nitrogen atmosphere to minimise interactions with CO_2. For further details see Rochelle et al., 1997 in Supporting Information).

Table 1
Chemical composition and pH of recipes for initial young near-field porewater (YNFP) and evolved near-field groundwater (ENFG) data to 3 significant figures (Rochelle et al., 1997). Charge is balanced by OH^-.

Chemical component	YNFP (mg l^{-1})	ENFG (mg l^{-1})
Na	1640	7730
K	3630	174
Ca	67.1	1980
Mg	–	–
Sr	–	174
Cl	–	11400
Br	–	25.2
CO_3	8.14	1.00
SO_4	–	1120
SiO_2	7.60	–
pH (at 70 °C)	11.8	10.9

The experiments were conducted as sacrificial batch experiments in stainless steel pressure vessels lined with Teflon® (Rochelle et al., 1997). Each 150 ml vessel was loaded under a nitrogen atmosphere with 35 g of rock and 140 g of fluid. Non-reacting 'blank' experiments for both leachates were also run containing approximately 100 g of fluid in 100 ml vessels. The cells were held in an oven at 70 °C ± 0.5 °C and shaken regularly by hand to achieve mixing.

The experiments reported here were sampled after 15 years and 4 months in a CO_2 controlled anaerobic chamber, with a hydrogen–nitrogen atmosphere. Solution samples were filtered to <0.2 μm with a nylon filter. A sub-sample of the solution was then immediately acidified (with 2% HNO_3) for cation analysis and another frozen (−20 °C) for anion analysis. Suspended fines were collected by preserving the 0.2 μm filter papers inside a CO_2 free desiccator. The pH and Eh of the filtrates were measured at the point of sampling at room temperature within the anaerobic chamber.

Cation concentrations in the solutions were analysed by Inductively Coupled Plasma Atomic Emission Spectroscopy (ICP-AES) using a Perkin–Elmer Optima 5300 dual view system. Ion Chromatography (IC) was carried out to quantify anion concentrations using a Dionex DX120 ion exclusion system with a Dionex ICE AS1 column for carbonate analysis and a Dionex AS9-HC column for all other anions. During the 15 years of reaction some experimental fluid evaporated and the extent of this has been estimated using the change in Cl^- (expected to be a conservative species) concentration over time. In the ENFG Cl^- concentration increased at the same rate in both the reacted and blank solutions (Table S1) and indicated approximately 34% fluid loss. In the YNFP system it was not possible to use Cl^- due to its very low concentration. However, a similar level of evaporation was observed in all the experiments, therefore it was assumed that 34% of the fluid was lost from every experiment and the data are corrected for this (Table S2). BET surface area analyses of the reacted rock and a sample of unaltered rock were performed using a Micromeritics Gemini V Surface Area Analyser. Quantitative analysis of the bulk mineralogy and the <2 μm size fraction of the altered and unaltered samples were determined by powder X-ray Diffraction (XRD) using a PANalytical X'Pert Pro series diffractometer, in conjunction with Rietveld refinement (for sample preparation and data analysis details see Supporting Information).

The rock samples were imaged using an FEI QUANTA 600 environmental scanning electron microscope (ESEM) and an FEI QUANTA 650 field emission gun ESEM (FEG-ESEM) both equipped with Oxford Instruments INCA 450 energy dispersive X-ray (EDX) microanalysis systems with a 50 mm X-Max silicon drift detector (SDD). The reacted solids and the particles retained on the 0.2 μm filter papers were imaged uncoated under low vacuum. Sections through the solids were created by embedding samples in resin and polishing under ethane-2-diol. These were then viewed uncoated under low vacuum and coated with 2.5 nm of carbon under high-vacuum. Transmission electron microscopy (TEM) with EDX and selected area electron diffraction (SAED) was conducted using an FEI Tecnai TF20 FEG-TEM with an Oxford Instruments INCA 350 EDX system with 80 mm X-Max SDD detector and a Gatan Orius SC600A CCD camera. Samples were prepared for TEM by ultrasonication in ethanol to create a suspension which was then deposited onto copper TEM grids with holey carbon films.

U(VI) reaction with unaltered rock, and 15 year reacted samples from the YNFP and ENFG systems was also examined. 0.1 g of the unaltered and reacted solids were each reacted in 35 ml of a 0.1 M NaCl solution (pH 7.0; representative of a simplified saline groundwater) with UO_2^{2+} spiked to a concentration of 3 mgl^{-1} under N_2. The suspensions were then agitated for 24 h prior to sampling. The solutions were filtered to $\leqslant$0.45 μm (nylon filter) and acidified (1% HNO_3), while the solids were frozen moist at −80 °C. The solutions were analysed by inductively coupled plasma mass spectroscopy (ICP-MS) for uranium concentration. From these data, distribution coefficient (K_d) values for U(VI) sorption (assuming no U(VI) phase precipitation) were calculated according to Eq. (4) (Fetter, 1999), where C^* is the mass of solute sorbed per dry unit weight of solid (mg kg^{-1}) and C is the concentration of solute in solution in equilibrium with the solid (mg l^{-1})

$$C^* = K_d C \quad (4)$$

The speciation of U associated with the rock samples was analysed using X-ray absorption spectroscopy (XAS). For this, the moist solid samples (~50% moisture) were mounted in double contained cells. Uranium L_{III}-edge XAS spectra were collected at beamline B18 of the Diamond Light Source. The data were collected in fluorescence mode using a 9 element Ge solid state detector at room temperature. Standards were collected in transmission mode for schoepite (U(VI)) and uraninite (U(IV)). The software package Athena (Ravel and Newville, 2005) was used to average multiple scans for each sample to improve the signal to noise ratio of the data and for background subtraction.

3. Results

3.1. Solution chemistry

After 15 years, the pH of the reacted YNFP and ENFG solutions were 9.9 and 8.8, respectively, while those of the corresponding 'blank' solutions remained at 13.3 and 12.2 respectively. The Eh of the reacted YNFP and ENFG solutions were +112 mV and +258 mV respectively, and those of the corresponding 'blank' solutions were +28 mV and +90 mV respectively, indicating the experimental solutions remained oxic throughout the experiment.

The Na, K, Ca, Mg, Si, CO_3, Sr and SO_4 concentrations of all the solutions at 15 years (corrected for evaporation) are shown in Fig. 1 along with the data for 0, 4, 9 and 15 months of reaction (Rochelle et al., 1997). Al concentration was <0.5 mg l^{-1} after 15 years of reaction and in all but the starting solutions (Rochelle et al., 1997). The concentrations of K and Na did not change between 15 months and 15 years of reaction (see Fig. 1 a and b). Ca, Si, Sr and SO_4 concentrations decreased in both leachates over the same period (see Fig. 1c–f). However, differences in the Mg and CO_3 concentrations existed between the two leachates. After 15 years Mg concentration was elevated in the ENFG, and CO_3 concentration was elevated in the YNFP (see Fig. 1g and h). It is highlighted that the solution concentration of Mg in the YNFP and ENFG is very low (<0.01 mg l^{-1}) up to 15 months, with the exception of the concentration in the YNFP at $t = 0$. It should also be noted that at 9 and 15 months of reaction, an elevated concentration (approx. 40 mg l^{-1}) of CO_3 was measured in the ENFG solution blank. However, as these levels were not observed throughout the experiment, it was attributed to the ingress of atmospheric CO_2(g) during analysis.

3.2. Mineral alteration

Quantitative XRD analysis of the unaltered rock showed it comprised of quartz, dolomite, mica, orthoclase feldspar, calcite, hematite and anatase (Table 2). Note that it was not possible to distinguish between different mica/clay phases (e.g. muscovite, biotite and illite) and they are grouped into 'mica'. XRD characterisation of the 15 year altered fracture fill identified the same bulk solids, with the addition of halite in the ENFG system, which is an artefact of sample drying. The XRD data further indicate that relative to the unaltered material, the YNFP altered rock is enriched in calcite, from 2.6% to 6.4%, and depleted in dolomite from 29.5% to 23.7% (see Table 2). Data for the ENFG altered rock suggest a similar but less definitive trend in this system with an increase in calcite from 2.6% to 4.5%, and a decrease in dolomite from 29.5% to 28.5%. The proportions of the other minerals remain unchanged with the exception of an increase in 'mica' in the YNFP altered material. However, it should be noted that the error on these analyses are up to ±2.5%, therefore some of these changes may be within analytical error.

Further XRD characterisation of the fraction identified as 'mica' was undertaken by isolating the <2 μm size fraction from the samples. In the unaltered rock, the clay minerals were identified as predominantly illite, with a trace amount of chlorite (Table 3) which confirms the findings of Rochelle et al. (1997). In the reacted YNFP and ENFG samples, XRD indicated that the predominant clay mineral was still illite. However, in the reacted samples, the patterns were characterised by broad, low intensity peaks centred on ~12.2 Å in the XRD pattern from the YNFP altered material and between 12.5 and 15 Å from the ENFG altered material. Following ethylene glycol-solvation a peak centred on ~17 Å appeared in the XRD patterns for both samples (Figs. S1 and S2). This suggests the presence of swelling clay, not present in the unreacted material, which is more abundant in the YNFP altered material than the ENFG material (Table 3). NEWMOD-modelling of the XRD data (Reynolds and Reynolds, 1996) from the YNFP altered material suggested that this interstratified illite/smectite consisted of 80% smectite, 20% illite phase. The absence of a peak at ~14 Å also suggests that there is no significant chlorite present in the altered samples.

Characterisation of the minerals using SEM revealed that the rock grains reacted for 15 years in both the YNFP and ENFG retained their angular shape and 125–250 μm size distribution indicating that no large scale dissolution or precipitation has occurred (Fig. S3).Dolomite reacted in YNFP for 15 years showed extensive pitting, indicating dissolution of the mineral surface (Figs. 3a and S4). However, examination of the material in section indicated the dissolution was limited to grain surfaces. Some dissolution of dolomite had been observed after 15 months of reaction, but to a much lesser extent than observed after 15 years (Rochelle et al., 1997). Euhedral, rhombohedral crystals of calcite, 5–10 μm in length, (Fig. 3b) were observed on silicate grain surfaces. This is thought to be secondary as calcite is not observed with this euhedral morphology in the early stages of the experiment (Rochelle et al., 1997).

After reaction in ENFG, grains of dolomite also exhibit surface pitting indicative of dissolution although to a much lesser extent than in the YNFP altered material (Fig. 2c and d). As in the YNFP system $CaCO_3$ crystals with rhombohedral morphology were observed on silicate mineral surfaces and are also identified as secondary calcite. However, in the ENFG system $CaCO_3$, identified as calcite, was also observed as poorly developed crystal coatings on dolomite grains (Fig. 2d). These coatings were not present on the unaltered dolomite or the material reacted for up to 15 months (Rochelle et al., 1997).

The surfaces of the quartz and feldspar altered in YNFP were completely coated with secondary phases with 'sheet-like' and acicular morphologies (Fig. 3a). The sheets were typically several micrometers in size (see Fig. 3b) and the needles several micrometers in length and <0.5 μm in width. EDX showed these

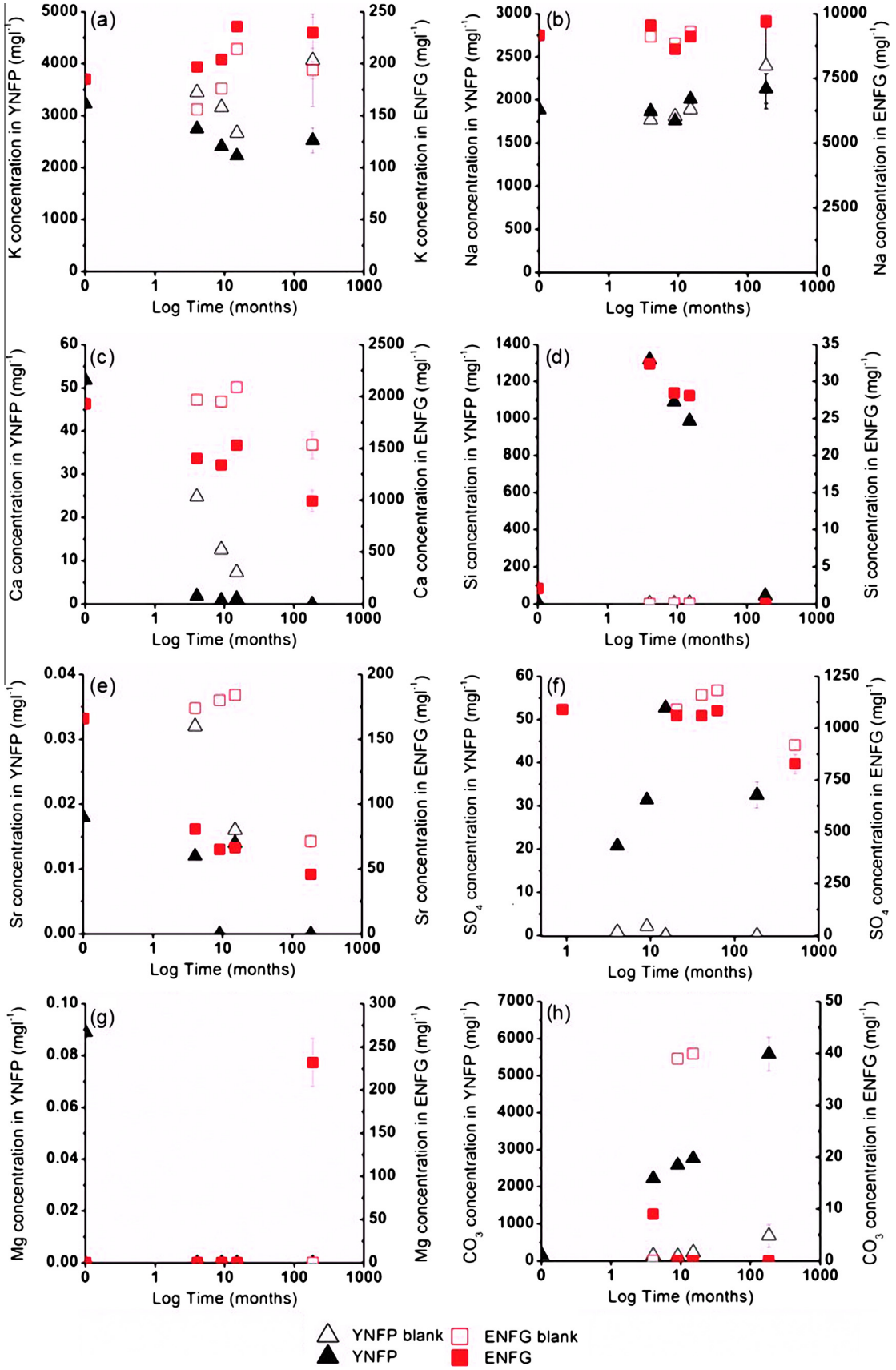

Fig. 1. Concentrations of (a) K, (b) Na, (c) Ca, (d) Si, (e) Sr, (f) SO_4, (g) Mg and (h) CO_3 in solution in the starting solution and after 4, 9, 15 months and 15 years of reaction in YNFP and ENFG (solid triangle and square markers respectively) and in corresponding 'blank' experiments (corresponding unfilled markers).

Table 2
Quantitative XRD analyses of the bulk mineralogy of the rock altered in YNFP and ENFG for 15 years and a sample of unreacted rock ('mica' represents undifferentiated mica/clay species and may include muscovite, biotite, illite etc.).

Mineral	Unreacted material (weight%)	YNFP altered sample (weight%)	ENFG altered sample (weight%)
Quartz	41.3	39.1	39.3
'Mica' (muscovite/biotite/illite etc.)	12.8	15.9	13.0
Dolomite	29.5	23.7	28.5
Calcite	2.6	6.4	4.5
Orthoclase	11.9	12.9	11.9
Hematite	1.7	1.7	1.6
Anatase	<0.5%	<0.5%	<0.5%
Halite	nd	nd	1.0

Table 3
Summary of the clay minerals identified through XRD analysis in the <2 μm size fraction of unaltered and YNFP and ENFG altered rock after 15 years of reaction.

	% Of <2 μm fraction mineral assemblage		
	Unreacted material	YNFP altered sample	ENFG altered sample
Illite	99	76	96
Chlorite	1	<1	1
Interstratified illite/smectite	nd	24	3

particles contained Mg, Al, K and Si and, coupled with their morphology, indicated they were aluminosilicate clays, potentially the interstratified illite/smectite clay phases identified via XRD.

The aluminosilicate surface coatings on the YNFP altered rock were further examined using TEM to eliminate interferences from the underlying primary mineral grains. The most abundant phase exhibited a 'sheet-like' morphology with particles ranging from 100's of nm to a few μm in size (Fig. 4a). Typically, this was identified via EDX as an Mg–silicate, though low levels of additional K and Fe were noted in a few examples of this phase. SAED patterns for these particles show the typical hexagonal pattern indicative of sheet silicate structured phases (Fig. 4a), and together with the EDX identify this phase as talc ($Mg_3Si_4O_{10}(OH)_2$). Two acicular morphology phases were also identified; (i) elongate rods approximately 100 nm in width and several μm in length, identified as a Mg–Al–silicate based on EDX analysis and exhibiting the typical hexagonal SAED pattern indicative of aluminosilicate clays (Fig. 4b), and; (ii) shorter rods approximately 100 nm in width and <1 μm in length, identified by EDX as a Mg–Al–K–silicate (Fig. 4c). There was also a phase which consistently occurred as groups of radiating acicular needles forming a 'sheet-like' morphology up to 2 μm in size (Fig. 4d). EDX indicated this phase was an Mg–Al–K–silicate with low and variable Fe content.

SEM analysis of the ENFG altered rock also revealed surface coatings of aluminosilicate clay particles on the primary silicate grains, similar to those observed in the YNFP altered system (Fig. 5a). These coatings comprised of particles with either 'sheet-like' or elongate

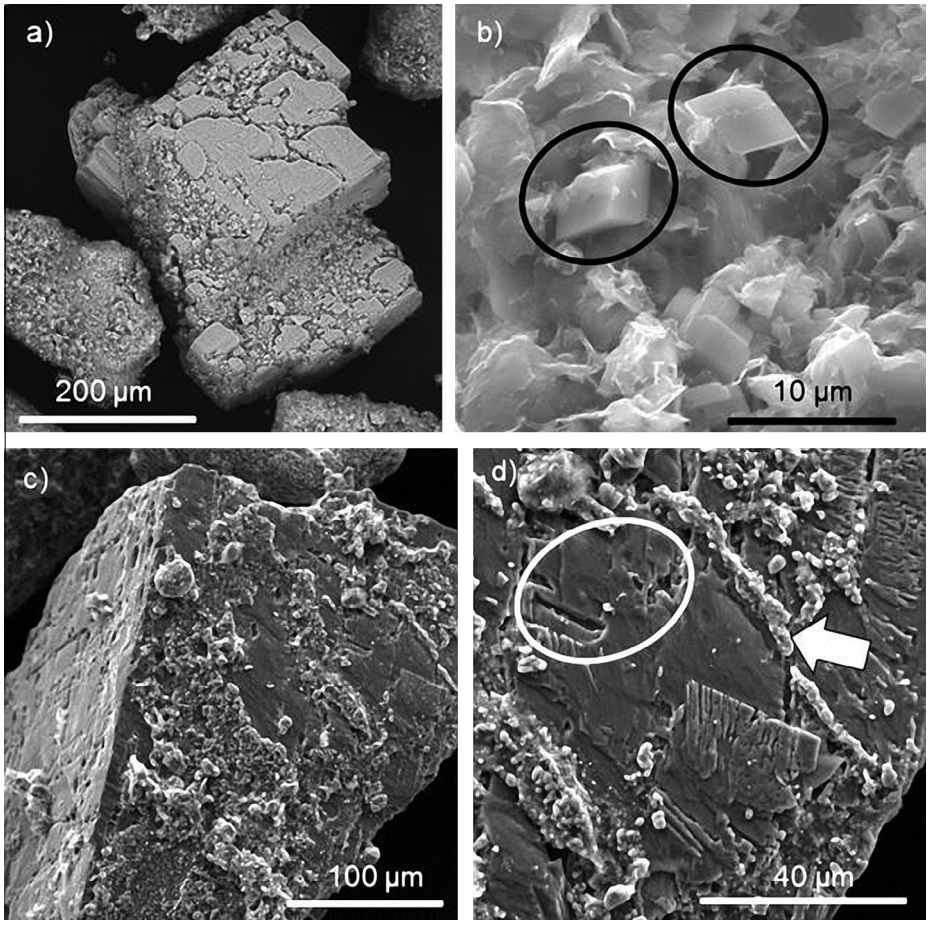

Fig. 2. SEM images of dolomite altered for 15 years: After reaction with YNFP (a) dolomite grain surface pitting, (b) calcite rhombs (highlighted in black ovals) on silicate grain surface. After reaction with ENFG (c) dolomite grain exhibiting minor pitting and a $CaCO_3$ coating of limited extent, (d) detail of pitting on dolomite grain surface (highlighted in the white circle) with $CaCO_3$ on surface indicated by the white arrow.

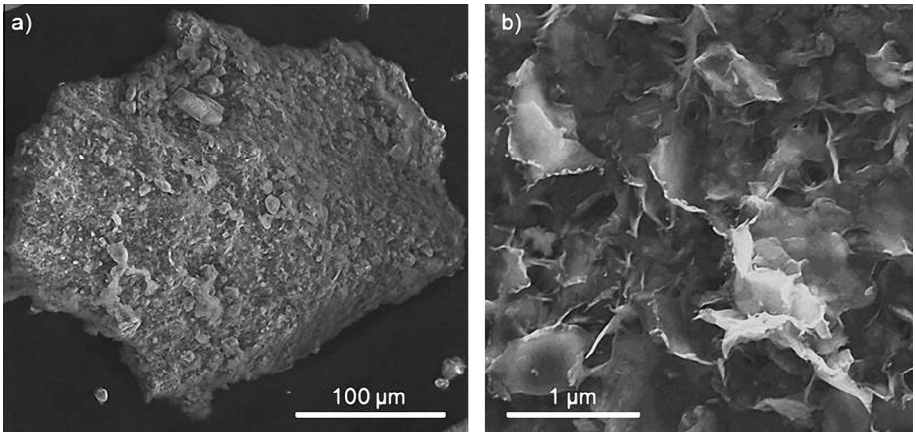

Fig. 3. SEM images from YNFP altered material of (a) a silicate mineral grain fully coated with secondary phases, (b) detail of silicate grain surface coating showing 'sheet-like' phase.

needle morphologies (Fig. 5b) and EDX showed they contained Mg, Al, K and Si. Detailed characterisation of individual particles using TEM discriminated several different phases. The predominant phase exhibited a 'sheet-like' morphology with particles ranging from 0.1 to 1 µm in size, composed of pure Mg–silicate which were identified as talc. The elongate particles had two distinct morphologies, elongate rods (approximately 100 nm in width and several µm in length, e.g. Fig 5c), and short rods (approximately 100 nm in width and <1 µm in length, e.g. Fig. 5d) which were both identified as Mg–Al–K–silicates using EDX. The Mg, Al and K content of all the particles varied significantly, though all three elements were always present with minor Fe also present in some examples (Fig. 5c and d). It is believed that these Mg–(Al)–(K)–silicate phases, identified in both the YNFP and ENFG altered rock, correspond to the interstratified illite/smectite clay phase indicated in the XRD analyses, most likely a mixture of Mg-rich smectite (e.g. Mg–rich saponite–K) and interstratified illite/smectite.

Analysis of the particles suspended in the both the reacted YNFP and ENFG solutions via SEM showed that they include fragments of primary orthoclase feldspar and quartz but were predominantly made up of a phase with 'sheet-like' morphology, 10–40 µm in size and of pure Mg–silicate composition (Fig. S5). This phase was identified as talc and was similar to the talc found as grain coatings in the material altered in both fluids.

In the ENFG altered rock, two additional minor secondary minerals were identified. The first occurred as groups of interlocking plates, up to 2 µm in size, containing predominantly Fe and Si hosted on silicate mineral surfaces (Fig. 6a). More detailed investigation of this phase using TEM confirmed this morphology and chemistry (Fig. 6a and b) which are indicative of the smectite mineral nontronite ($(Ca_{0.5},Na)_{0.3}Fe_2^{3+}(Si,Al)_4O_{10}(OH)_2{\cdot}nH_2O$). The second phase occurred as euhedral, tabular, lath shaped crystals, 50–100 µms in size, with pitted surfaces (Fig. 6c). Chemically this phase was found to contain Sr and S (Fig. 6d) and based on chemistry and morphology is identified as celestite ($SrSO_4$). Neither of these phases was identified in the unreacted material and nontronite was not found up to 15 months of reaction (Rochelle et al., 1997). It is believed that the strontianite observed in the ENFG reacted material up to 15 months of reaction (Rochelle et al., 1997) was in fact the celestite identified in this study as the crystals were the same size, exhibited the same morphology and were Sr-rich. However, up to 15 months of reaction the crystals were not pitted (Rochelle et al., 1997).

In summary, the altered solids from both leachate systems were found to be similar. In both systems evidence for dolomite dissolution and secondary calcite formation was observed. However, the predominant secondary phases formed in both systems were an assemblage of Mg–(Al)–(K)–silicates of varying chemical composition and morphology. These phases were identified as talc, Mg-rich smectite (e.g. Mg–rich saponite–K) and Mg-rich interlayered illite/smectite phases. As expected, the magnitude of these alteration features were less extensive in the less aggressive ENFG system and additional minor secondary phases of nontronite and celestite were observed in this more chemically complex system. Interestingly, SEM and TEM analyses did not identify C–S–H phases or appophyllite–KOH in the materials reacted for 15 years in the YNFP or ENFG experiments although these were pervasive in the altered BVG up to 15 months of reaction (Rochelle et al., 1997).

3.3. U(VI) sorption

To assess whether alteration affected the absorption properties of the rock, the reaction of U(VI) with unaltered, and 15 year altered rock samples was studied. The surface areas of the unaltered and YFNP and ENFG 15 year altered rock were determined to be 5.31, 6.04 and 4.93 $m^2\ g^{-1}$ (±3%), respectively, and indicated that any differences in sorption capacity between the samples was unrelated to surface area.

The concentrations of U(VI) in solution following the adsorption experiments (see Table 4) indicate that less than 6% of the U(VI) was taken up by the unaltered BVG and 30% and 40% was taken up by ENFG and YNFP altered material, respectively.

The calculated *Kd* values for both 15 years reacted rock samples are an order of magnitude greater than the unaltered material (Table 4). Assuming no U(VI) phases have precipitated (no evidence for discrete U(VI) minerals was observed), this indicated that the secondary phases or altered primary mineral surfaces have a higher sorption capacity for U(VI) than the unaltered rock. Interestingly, the *Kd* of the YNFP altered system was modestly elevated compared to that of the ENFG altered system, suggesting greater U(VI) retention on this sample. This indicates that the secondary phases/altered surfaces created during alteration are key to U(VI) adsorption and that the extent of alteration directly correlates with U(VI) uptake.

Comparison of the size, shape and positions of the peaks in the uranium X-ray absorption near edge spectroscopy (XANES) spectra from the samples with those from the standards indicated that the U(VI) sorbed to the rock samples has the same local bonding environment as U(VI) in schoepite (Fig. 7). This indicates that the uranium is present as U(VI) coordinated by six oxygen atoms, two axial oxygen atoms at ~1.8 Å and four equatorial oxygen atoms at ~2.4 Å, in a standard uranyl geometry (Grenthe et al.,

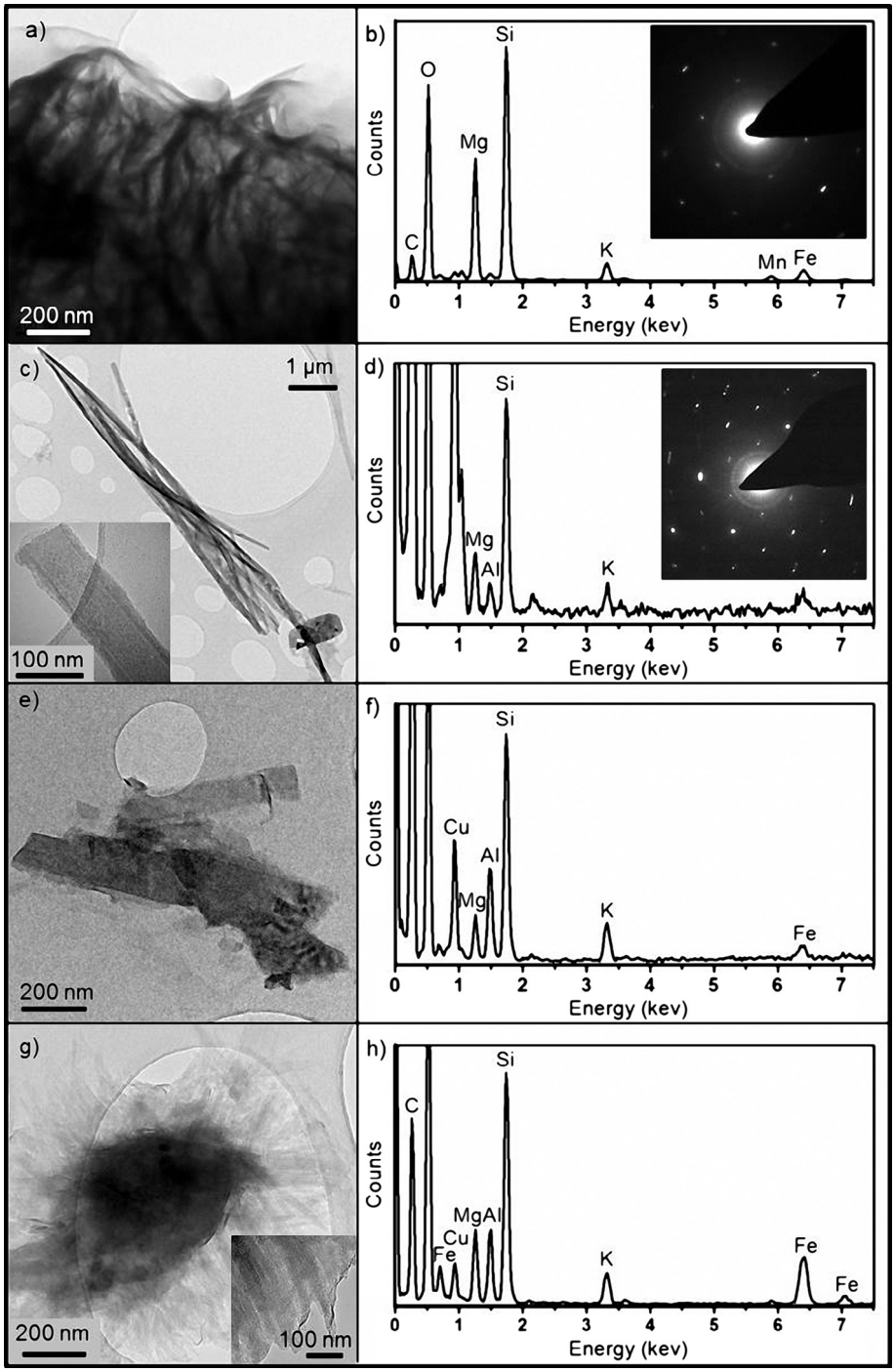

Fig. 4. Surface phases from rock altered in YNFP for 15 years (a) Mg–silicate 'sheet-like' phase: TEM image and (b) corresponding EDX spectrum and SAED pattern; (c) Mg–Al–silicate elongate rods: TEM image with inset higher resolution of rod end, (d) corresponding EDX spectrum and SAED pattern; (e) Mg–Al–K–silicate short rods TEM image and (f) corresponding EDX spectrum; (g) group of radiating rods of Mg–A–K–silicate composition TEM image with inset showing the 'sheet-like' nature of the group of radiating acicular needles and (h) corresponding EDX spectrum.

2008; Burns et al., 1997). These XANES spectra and U speciation are consistent with other studies of U(VI) adsorption at neutral pH to a range of mineral phases e.g. clay (Schlegel and Descostes, 2009) and goethite (Sherman et al., 2008) which support the conclusion that uranium was adsorbed to the surface of the rock fragments. Due to the low concentration of U(VI) associated with the samples, it was not possible to collect extended X-ray absorption fine structure (EXAFS) data of sufficent quality in the time available required for further interpretation of the U(VI) coordination environment.

4. Discussion

This investigation identified significant changes in both the mineralogy of the BVG rock and cement leachates after 15 years of reaction and demonstrated that this had an impact on radionuclide retention. However, in order to understand the evolution of these systems, it is necessary to discuss the results of this study in with those from the first 15 months of the reaction as reported by Rochelle et al. (1997). In summary, during the first 15 months of reaction poorly-ordered C–(A)–(K)–S–H phases and minor

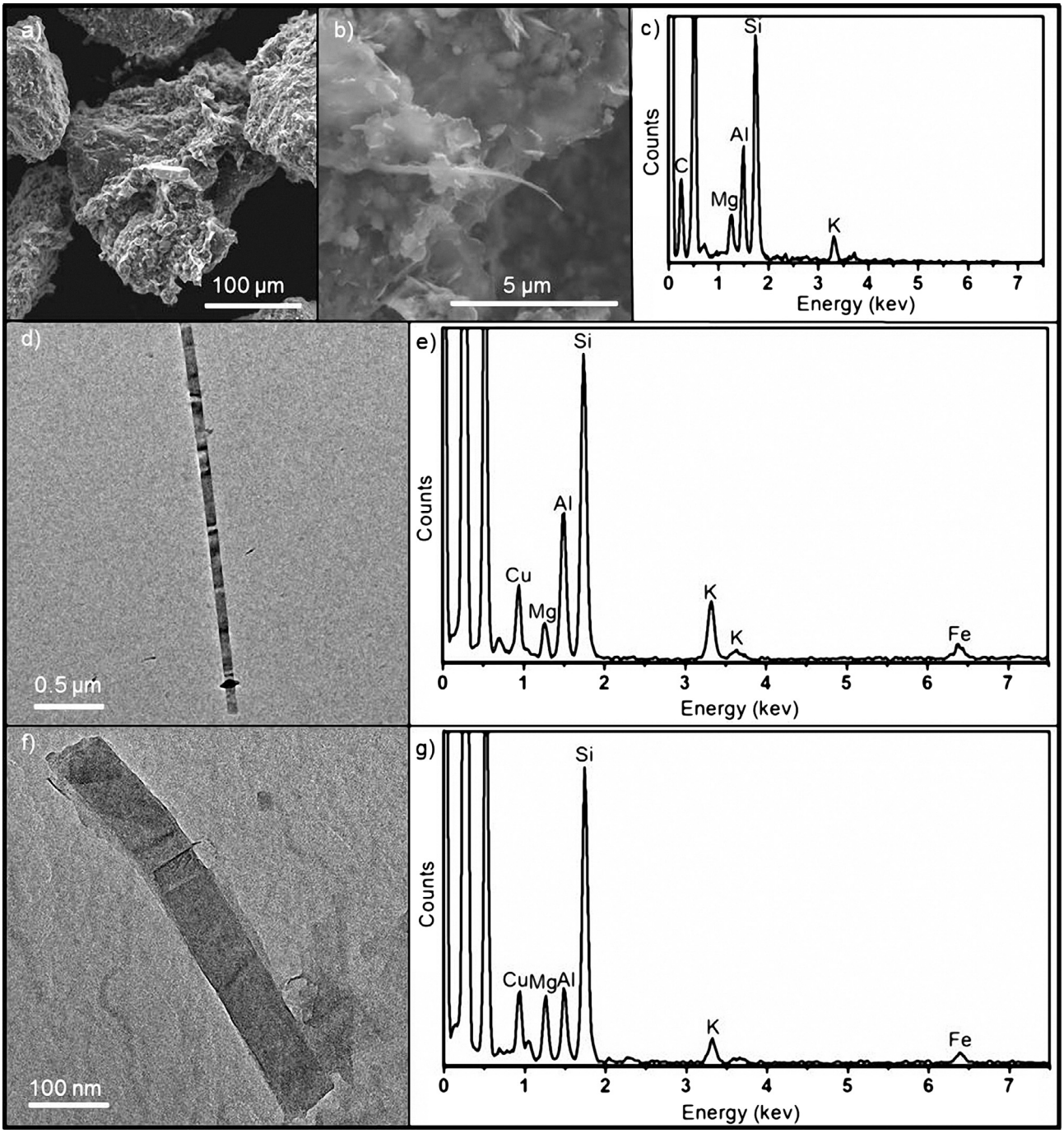

Fig. 5. Surface phases from rock altered in ENFG: (a) Silicate grain coated with secondary Mg–(Al)–(K)–silicates, (b) detail of the silicate grain coating exhibiting 'sheet-like' and elongate needle morphologies (c) EDX spectrum collected via SEM of coating in b, (d) Mg–Al–K–silicate elongate rod, (e) EDX spectrum collected via TEM correlating to phase shown in e, (f) Mg–Al–K–silicate short rod and (g) EDX spectrum collected via TEM correlating to phase shown in f.

secondary appophyllite–KOH formed in both the YNFP and ENFG. However, between 15 months and 15 years of reaction the solution composition of both the YNFP and ENFG changed significantly and a different secondary mineral assemblage stabilised. This demonstrated that continued chemical and mineralogical evolution occurred and indicated a change in the reaction processes in these systems. Importantly, between 15 months and 15 years, two interconnected reactions occurred: firstly, dedolomitisation; and secondly, the transformation of C–(A)–(K)–S–H and illite to Mg-bearing aluminosilicate clays. These processes are discussed in detail below.

4.1. Dedolomitisation

Electron microscopy and quantitative XRD show the dissolution of dolomite and formation of secondary calcite, providing evidence that dedolomitisation occurred (Eq. (3)). In addition, changes in solution compositions were indicative of dedolomitisation. In the YNFP carbonate concentration increased from 166 mg l^{-1} in the original solution to 5070 mg l^{-1} after 15 years of reaction (Fig. 1h). The gradual increase in CO_3 concentration throughout the experiment (Fig. 1h) is attributed to dedolomitisation, and may correlate with the minor amount of dolomite dissolution

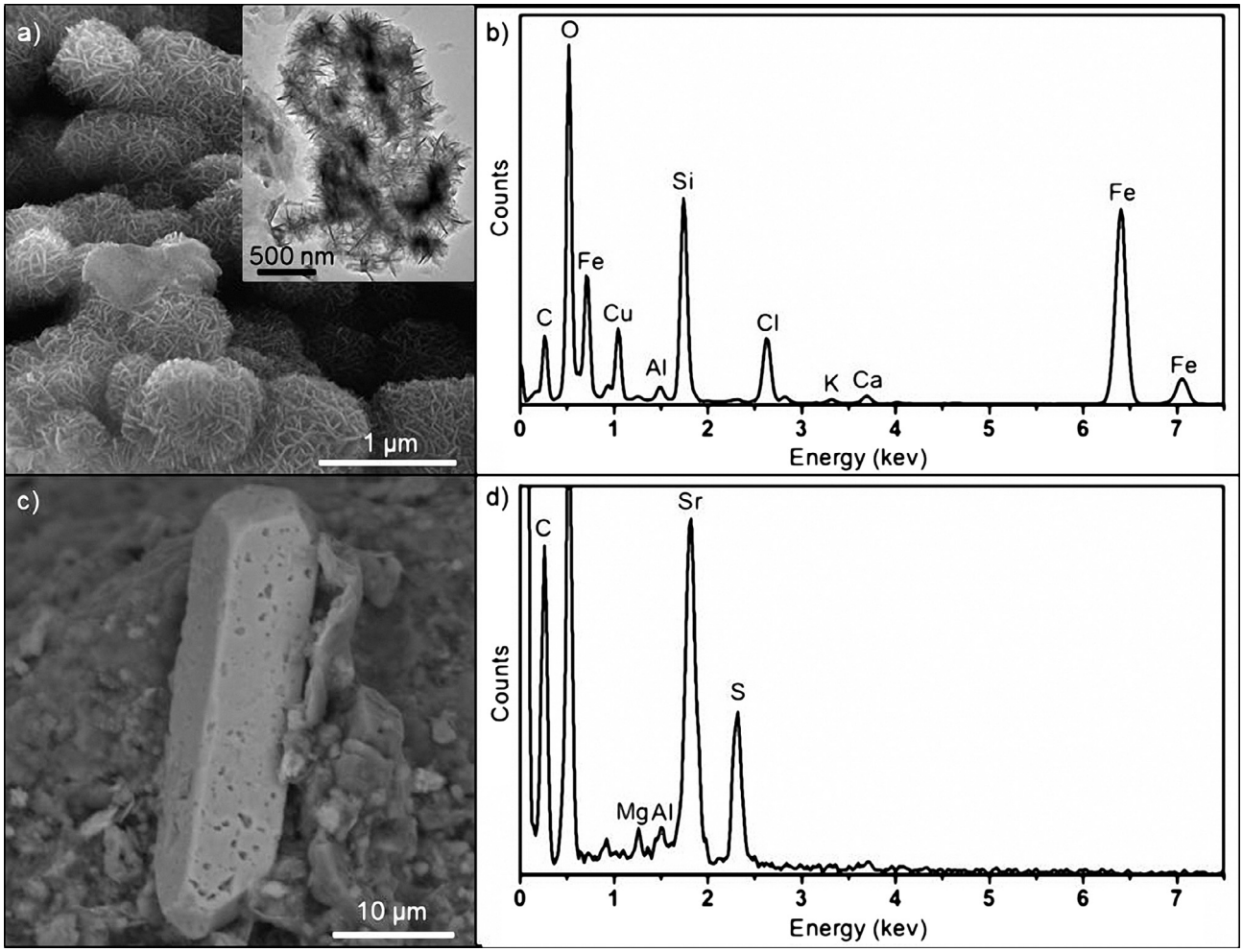

Fig. 6. (a) scanning electron micrograph of nontronite on a silicate grain surface with inset TEM image, (b) EDX spectrum taken via TEM, (c) scanning electron micrograph of pitted celestite (d) EDX spectrum corresponding to phase shown in c.

Table 4
Concentration of U(VI) (to 2 s.f.) remaining in solution after 24 h equilibration with BVG in a 0.1 M NaCl solution spiked with 3 ppm U(VI), the percentage of U(VI) adsorbed (to 2 significant figures) and the corresponding distribution coefficient (Kd) values.

	Unaltered	Altered in YNFP	Altered in ENFG
U(VI) in solution (mgl^{-1})	2.8 ± 0.06[a]	1.8 ± 0.04[a]	2.1 ± 0.06[a]
% U(VI) adsorbed	6.7	40	30
Kd (lkg^{-1})	714	6670	4290

[a] Error is 1 standard deviation from the mean (triplicate analyses).

observed at the beginning of the experiment (Rochelle et al., 1997). The same increase in carbonate concentration was not observed in the ENFG system (Fig. 1f). However, as the concentration of Ca^{2+} in the ENFG is high, any CO_3 released through dedolomitisation would rapidly form $CaCO_3$. Dedolomitisation would also release significant amounts of Mg^{2+}. Evidence for this is observed in the ENFG system ($[Mg^{2+}] > 200$ ppm at 15 years), but the concentration of Mg^{2+} in the YNFP remains low, <1 mg l^{-1} throughout the experiment. This is attributed to either the low solubility of Mg^{2+} in highly alkaline solutions (Baes and Mesmer, 1976) and/or the rapid uptake of Mg^{2+} into secondary clay phase formation (see Section 4.2).

The dedolomitisation reaction consumes hydroxyl ions (Eq. (3)) and is therefore favoured at high pH (Min and Mingshu, 1993). However, as only minor dedolomitisation was observed at high

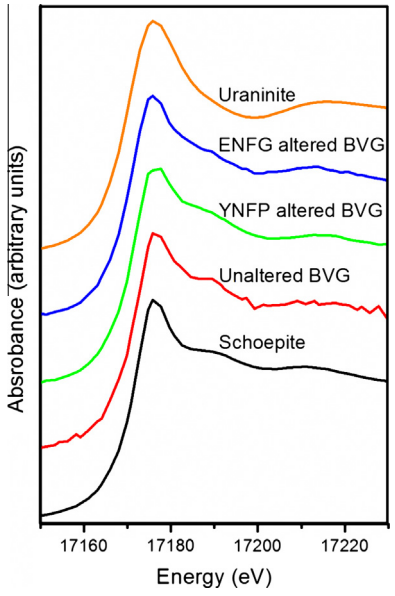

Fig. 7. Uranium L_{III} XANES spectra of schoepite (U(VI) reference), uranium sorbed to unaltered BVG, uranium sorbed to BVG altered in YNFP, uranium sorbed to BVG altered in ENFG and uraninite (U(IV) reference).

pH up to 15 months we can say that the rate of this reaction was restricted in the systems studied. This highlights the importance of longer term (>10 years) experimental studies to fully resolve the chemical and mineralogical reactions occurring in the CDZ. Thermodynamic predictions suggest that dedolomitisation would not occur below pH 11 (Min and Mingshu, 1993). As pH had decreased below 10 in the ENFG by 15 months of reaction (Rochelle et al., 1997) dedolomitisation would likely be restricted during the latter stage of the experiment. However, a high Ca^{2+} concentration, as found in both leachates, has been shown to promote dedolomitisation at lower pH, for example at cement–dolomite aggregate interfaces in concrete (Min and Mingshu, 1993). The enhancement of dedolomitisation occurs as Ca^{2+} reacts with aqueous CO_3^{2-} released in dedolomitisation to form $CaCO_3$ effectively removing CO_3^{2-} from solution and so driving the dedolomitisation reaction. Accordingly, the occurrence of dedolomitisation in the latter stage of this experiment is attributed to the presence of aqueous Ca^{2+} in the cement leachates. This suggests that this reaction will always be favoured in the CDZ.

4.2. Mg–silicate formation

Examination of the reacted fracture fill showed that after 15 years, in both leachate systems, grains were coated with secondary Mg–(Al)–(K)–silicate minerals, most likely a mixture of talc, smectite (Mg–rich saponite–K) and interstratified illite/smectite. Similar Mg-rich solid phases have been observed previously as minor components in high pH clay alteration experiments/analogues. For example, saponite was recognised as an alteration product of bentonite by Cuevas (2004), secondary Mg-enriched mineral phases have been observed at the Tournemire analogue site (Tinseau et al., 2006; Techer et al., 2012) and palygorskite was identified as an Mg-rich alteration product of bentonite by high pH groundwaters in the Troodos natural analogue site (Alexander et al., 2012). The formation of these phases at these high pH conditions is not unexpected as they are commonly associated with alkaline, saline lake environments (Yeniyol, 2007, 2012; Hojati et al., 2010; Akbulut and Kadir, 2003) where they form from post-sedimentary alteration of soils and rocks in high pH fluids in the presence of dolomitic material (Derkowski et al., 2013; Xie et al., 2013; Schwarzenbach et al., 2013; Birsoy, 2002). Their formation has also been identified in cement–aggregate systems where dedolomitisation in the presence of $Ca(OH)_2$ and amorphous silica resulted in the formation of a mixed calcium–magnesium silica gel (Gali et al., 2001).

The presence of secondary Mg-bearing phases provides further evidence of dedolomitisation as dolomite is the major source of Mg^{2+} in the rock. However, dedolomitisation generally results in the production of brucite ($Mg(OH_2)$) (see Eq. (3)), which was initially found as a minor reaction product up to 15 months of reaction, but was not identified after 15 years. We suggest that this is due to the preferential reaction of the released Mg^{2+} to form the secondary Mg–(Al)–(K)–silicates. This has been observed in high pH cement systems where the presence of aqueous Mg and Si results in the formation of hydrated magnesium silicates such as talc–serpentine group minerals (Glasser, 2001; Eglinton, 2006). We propose that two independent reaction pathways result in the assemblage of secondary solid phases observed. Firstly, the reaction of Mg^{2+} released by dedolomitisation with aqueous silica to form the pure Mg–silicate, talc, by direct precipitation, as shown in Eq. (5).

$$3Mg^{2+} + 4H_3SiO_4^- + 2OH^- \Rightarrow Mg_3Si_4O_{10}(OH)_2 + 6H_2O \quad (5)$$

This is evidenced by the decrease in aqueous Si concentration in solution between 15 months and 15 years of reaction in both the YNFP and ENFG fluids (see Fig. 1d), and the occurrence of talc in suspension which is indicative of formation through direct precipitation from solution. Secondly, the reaction of Mg^{2+} with primary illite and early formed C–(A)–(K)–S–H leading to transformation to Mg–(Al)–(K)–silicates. The transformation of illite to smectite (i.e. Mg–rich saponite–K) is likely to occur via an interstratified illite/smectite clay. Such interstratified clays are known to form as intermediate phases during the transformation of clay minerals (Cuadros et al., 2010). In this study the high pH and Mg^{2+} concentrations may have led to the transformation of illite either via cation exchange reactions and/or dissolution and precipitation. In addition, the absence of any C–(A)–(K)–S–H after 15 months of reaction shows that these phases have also either dissolved or transformed during the latter stages of the experiment. The transformation of C–S–H as a result of dedolomitisation has been suggested in numerical simulations of cement–aggregate systems; the release of CO_3^{2-} from dolomite results in calcite precipitation at the expense of the Ca content of C–S–H, and Mg^{2+} substitutes into the C–S–H structure eventually forming Mg–silicates (Gali et al., 2001). We proposed that this process is responsible for the destabilisation of the C–(A)–(K)–S–H formed in the early months of this experiment, and further promoted the dedolomitisation reaction by removing CO_3^{2-} from solution.

4.3. YNFP and ENFG comparison

Qualitatively, the degree of primary mineral dissolution and secondary phase formation appears greater in the YNFP. This would be expected due to the YNFP's more aggressive, higher pH. However, despite the difference in solution composition, no significant difference was found in the assemblage of alteration phases produced in the two cement waters or in the surface area of the two samples. This indicates that broadly similar reaction processes have occurred in both systems, with the extent of alteration directly related to solution pH. In a real repository environment i.e. an open system, there would be a constant replenishment of cement pore water into the geosphere, therefore the observed decreases in pH and changes in solution composition would not occur to the same extent within the CDZ. This would increase the overall rate of the alkaline alteration reactions, but would be unlikely to significantly change which reactions occuring or the products formed. Two minor additional secondary phases, celestite and nontronite, were however identified in the ENFG system. Celestite precipitated from solution during the first 15 months of reaction (Rochelle et al., 1997) but surface pitting after 15 years indicated re-dissolution of this phase. As Sr^{2+} is known to substitute into calcite (Tesoriero and Pankow, 1996; Lorens, 1981; Pingitore and Eastman, 1986), and as calcite formed between 15 months and 15 years of reaction, it is proposed that Sr^{2+} substitution into calcite has driven celestite dissolution. Nontronite was not identified up to 15 months of reaction and Fe concentration in solution was generally below detection limits throughout the experiment as would be expected at highly alkaline pH. However, a significant proportion of the primary dolomite in the fracture fill is known to be ferroan (Rochelle et al., 1997). Therefore the occurrence of nontronite after 15 years of reaction is attributed to the reaction of Fe released from ferroan dolomite with dissolved silica via a similar mechanism to that which formed the secondary Mg-bearing aluminosilicate phases.

4.4. Geochemical modelling

Geochemical speciation and reaction-path modelling (PHREEQC, Parkhurst and Appelo, 2010) has been used to investigate the potential for dedolomitisation to produce the observed formation of Mg–(Al)–(K)–silicate phases in the experiments observed between 15 months and 15 years of reaction. Firstly, saturation

indices (SI) of mineral phases were calculated for the YNFP and ENFG aqueous compositions at 70 °C at 15 years using the Lawrence Livermore National Laboratory (LLNL) database, see Table S2 for aqueous composition considered and Table S3 for calculated saturation indices of oversaturated silicate and carbonate phases. In both YNFP and ENFG disordered dolomite is undersaturated, consistent with the observed dolomite dissolution. More crystalline forms of dolomite are oversaturated in both solutions. Calcite is oversaturated in YNFP consistent with its precipitation, but it is undersaturated in ENFG. It should be noted that measured carbonate concentrations considered in these calculations and hence calculated SI could be higher (more positive) than in the unopened experiment as CO_2 might have dissolved in the solutions on sampling. The model results confirm undersaturation of dolomite and oversaturation or equilibrium with calcite in YNFP consistent with dedolomitisation.

Considering silicates, for YNFP saponite phases with exchangeable K, Na, Ca and Mg, talc, phlogopite and chrysotile are the only silicate phases in the database that are oversaturated. Reaction-path calculations showed that phlogopite followed by chrysotile were the most stable phases. However, these phases are only likely to able to crystallise at high temperatures, e.g. above 100 °C. The oversaturation of saponite and talc is consistent with their observed formation in YNFP. Reaction-path calculation where talc and the saponite phases are allowed to precipitate predicted the precipitation of 2.1e−07 mol/kg water of saponite–K would form.

In the case of ENFG, experimental Al solution concentration after 15 years of reaction was below the analytical detection limit (Table S2). Therefore in this speciation calculation the limiting concentration of 0.01 mgl^{-1} Al was assumed in order to consider Al containing phases. A larger number of phases are oversaturated than for YNFP, which may be a consequence of the assumed Al concentration, although several high temperature pyroxene and olivine pure Mg silicate phases are thermodynamically stable at the lower pH of ENFG. Saponite and talc phases are again oversaturated, but the SI are higher than for YNFG. Interestingly brucite ($Mg(OH)_2$) is very close to saturation in ENFG (SI -0.04). Reaction path calculations that allow saponite and talc to precipitate resulted in the formation 1.1e−06 mol/kg water of Saponite–Mg and 1.4e−05 mol/kg water of talc. These speciation and reaction-path calculations on the YNFP and ENFG solution compositions confirm the dedolomitisation reaction and the associated precipitation of the Mg silicate phases saponite and talc, which drive the reaction (Eq. (5)).

To further examine the controls on talc or saponite precipitation in the experiments the dedolomitisation reaction was simulated as a Reaction with PHREEQC. In this reaction dolomite was reacted with C–S–H in both YNFP and ENFG fluid compositions reported at 15 months of reaction (Rochelle et al., 1997). C–S–H is represented in the reaction model as C–S–H-gel (Reardon, 1990, 1992) for which the thermodynamic data was added to the LLNL database (the thermodynamic data for all phases are given in Supplementary Information). Saponite and talc phases were allowed to precipitate during the reaction. For each solution two scenarios were examined (i) where the reaction occurred in solutions with no additional source of Al and (ii) where an additional source of Al was provided by muscovite representing the 'mica/illite' phase identified in the BVG.

In these models the extent of reaction is defined by the assumption that the reaction is driven by the rate and extent of dolomite dissolution. The difference in the weight% of dolomite in the unaltered and altered rock samples, identified by quantitative XRD (Table 2), indicates that over 15 years of reaction ~0.019 and ~0.001 mol of dolomite have dissolved in the YNFP and ENFG systems respectively. A constant rate of dedolomitisation was assumed; therefore the amount of dolomite dissolved between 15 months and 15 years can be calculated as 1.7×10^{-2} moles in the YNFP and 9.2×10^{-4} moles in the ENFG. The reaction was modelled at 70 °C and in order to examine the sequence of mineral precipitation products, it was divided into 18 equal reaction-steps. At each step the system was equilibrated with all components. As C–S–H was observed up to 15 months of reaction but not after 15 years, for the purpose of the model it is necessary to assume C–S–H dissolves during this time. Since there is no quantitative data for the amount of C–S–H formed in the experiment, the quantity of C–S–H dissolving in each leachate was estimated and refined using trial and error to get good agreement between the modelling results and experimental data for pH and Ca^{2+} concentration at 15 years of reaction. As a result it is assumed 2.1×10^{-4} moles and 1.1×10^{-5} moles C–S–H dissolve in the YNFP and ENFG, respectively. The solution chemistry and mineral SI evolution over time predicted by the model are summarised in Tables S4 and S5. Broadly, the modelled solution chemistry at 15 years of reaction is similar to the observed solution chemistry (same order of magnitude). However, modelled Si concentrations are higher and Mg concentrations are lower.

Throughout the modelled reaction the SI of dolomite and C–S–H are negative in both the YNFP and ENFG, in the presence and absence of a dissolving Al-bearing solid, indicating that these phases were undersaturated (the predicted SI of all phases over time in both leachates are provided in Supplementary Information). The amount of the solid reactants and precipitated secondary solid phases predicted to form in YNFP is shown in Fig. 8. Results for ENFG are provided in Supplementary Information.

In both leachates in the absence of a dissolving Al-bearing phase, (Fig. 8a) a very small amount of saponite forms initially, but talc is the main alteration product formed. In the case where muscovite is included in the model (Fig. 8b), saponite forms in preference to talc. The formation of talc where Al is limited is consistent with the observed occurrence of talc present as suspended particles in the experiment fluids. The formation of saponite associated with the presence of muscovite is consistent with the association of saponite and mixed layered illite–smectite with the BVG rock which provides a source of Al to stabilise saponite in preference to talc.

Approximately the same quantity of saponite is predicted to form in both YNFP and ENFG in the absence of muscovite and results also confirm the experimental observations that calcite and talc can form in both leachate systems (Figs. 8a and S6). In YNFP talc is the main secondary phase predicted to form in association with a minor amount of secondary saponite (Fig. 8a) while in ENFG saponite initially precipitates followed by talc (Fig. S6). The relative amounts of saponite–K and talc that form is related to the amount of K available for saponite–K formation. Interestingly, in ENFG saponite–Ca is predicted to form rather than saponite–K attributed to the significantly higher concentration of Ca in this fluid (Table S4). The model also reproduced the drop in pH observed in both leachate systems (Table S5). Overall, thermodynamic considerations show that dedolomitisation can lead to the transformation of silicate phases (i.e. C–S–H), leading to the formation of talc and saponite–K, which is in agreement with experimental observations.

4.5. Uranium sorption

The investigation of U(VI) sorption to the materials altered in this study indicated that, despite no significant detectable change in surface area, uranyl sorption to the BVG reacted at high pH for 15 years was greater than to unreacted BVG. This suggests alteration of the rock and the formation of secondary phases, including Mg–silicates, may increase the rock's sorption capacity for U(VI).

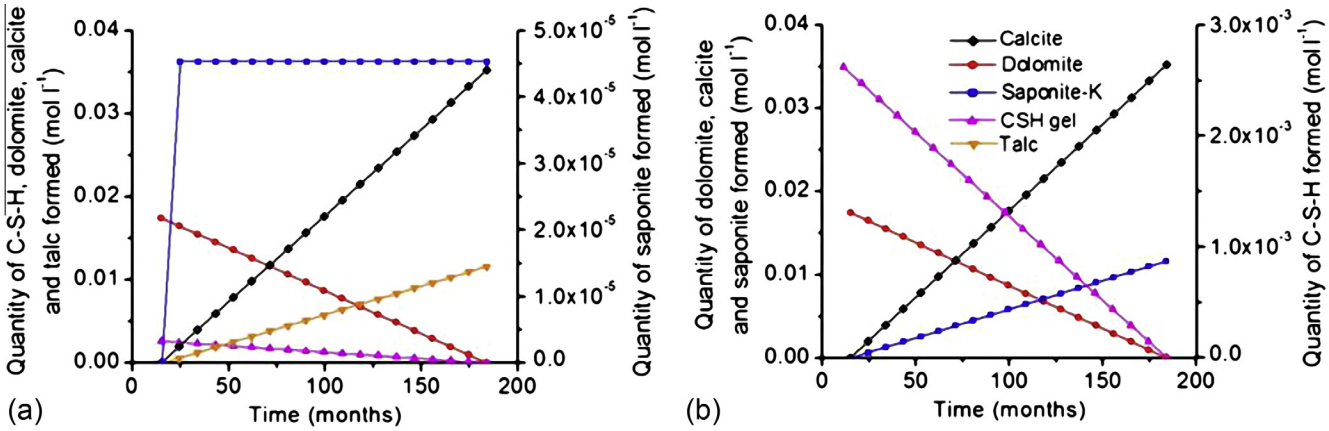

Fig. 8. Moles of (a) saponite–K, calcite, dolomite, C–S–H gel and talc in YNFP without muscovite and (b) saponite–K, calcite, dolomite, C–S–H gel and talc in YNFP in the presence of muscovite, predicted to form between 15 months and 15 years of reaction using PHREEQC modelling.

Results also show that sorption is modestly greater to the material reacted in YNFP than to that reacted in ENFG. This supports the hypothesis that the presence of secondary phases increases the sorption capacity of the rock as secondary phases are more abundant in the YNFP system. This indicates that long term, high pH mineral reactions could be beneficial for the geosphere as a barrier to radionuclide migration and highlights the need for further study of the secondary minerals formed in this study in relation to radionuclide transport.

5. Summary and conclusions

This study investigated the reaction of a fracture fill material with high pH cement leachates within 15 year laboratory experiments. As a result of the extended timescale of these experiments, two different phases of the alkaline rock alteration reaction were identified. In phase 1, a Ca–silicate dominated secondary mineral assemblage (i.e. containing C–S–H and apophyllite–KOH) stabilised as reported by Rochelle et al. (1997) (Fig. 9). Subsequently these initial phases destabilised and Mg–(Al)–(K)–silicates and calcite formed under the reaction conditions of this study (Phase 2 – Fig. 9). The evolution of the secondary mineral assemblage is attributed to a change in the dominant reactions between the early and late stages of the experiment. Initially, the high pH of the leachates caused the dissolution of primary silicate minerals and formation of C–(A)–(K)–S–H in the Ca^{2+} rich solutions (Rochelle et al., 1997). Between 15 months and 15 years of reaction (Phase 2) significant dedolomitisation occurred and the early formed C–(A)–(K)–S–H destabilised (Fig. 9) which led to the formation of secondary $CaCO_3$ and Mg–(Al)–(K)–silicates.

Previous studies of high pH-rock alteration have identified C–(A)–(K)–S–H, feldspars and zeolites as the dominant secondary phases likely to form in a GDF environment over time (e.g. Gaucher and Blanc, 2006; Savage, 2011). The formation of Mg–(Al)–(K)–silicates has only been suggested in a few studies of CDZ-type alteration as a minor product (Cuevas, 2004; Techer et al., 2012) and has not been widely considered. This study has shown that, in the presence of the common rock forming mineral dolomite, these phases may form and become the dominant secondary phases in a GDF scenario. An additional implication of this finding is that other sources of Mg^{2+} may exist at a GDF site (e.g. magnox fuel cladding within the waste) which could potentially contribute to the formation of secondary Mg–(Al)–(K)–silicates. This study also found that the secondary mineral phases resulting from high pH rock alteration may increase the rock's sorption capacity for U(VI).

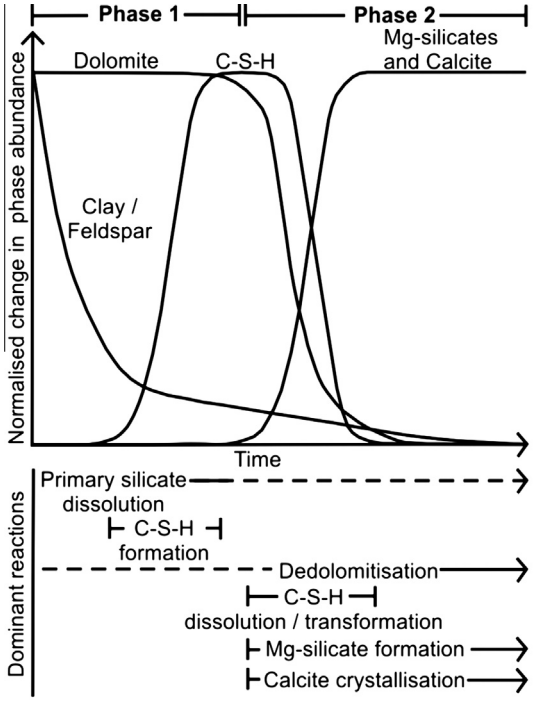

Fig. 9. Schematic diagram describing the general evolution of reaction proposed for this experiment.

At a broader level, the findings of this study illustrate that, in the CDZ around a GDF, there is potential for different mineral alteration reactions to occur over time. This may result in several different, transient mineral assemblages forming. The similar characteristics of the secondary phases produced in the two leachate systems studied here suggests that the alteration processes and resulting secondary mineral assemblages may not be significantly affected by the evolutionary stage of the cement leachate. However, the greater extent of alteration observed in the YNFP system, and the resulting increase in uranium sorption to the YNFP altered material observed, indicate that the composition of the leachate could impact radionuclide transport. Indeed, even at the relatively short timescale investigated here, the potential for significant mineralogical evolution has been demonstrated. It is also important to note that the Mg–clay mineral assemblage identified in this study cannot be shown to be a stable equilibrium assemblage, but may also be a metastable assemblage such as the C–S–H phases identified initially. The question is therefore raised as to whether

further reaction may be anticipated. This work has important implications for any GDF safety case and highlights the need for longer-term experimental programmes to be considered during the implementation of geological disposal, and the need to develop the experimental-modelling interface so that predictions of CDZ evolution are robust.

Acknowledgements

This study was supported by the Engineering and Physical Sciences Research Council (EPSRC) through the Nuclear Fission Research, Science and Technology (Nuclear FiRST) Doctoral Training Centre (DTC) (grant number: EP/G037140/1) via a studentship to Moyce and has been supported by the Natural Environment Research Council (NERC) through the Biogeochemical Gradients and RADionuclide transport BIGRAD project (grant numbers: NE/H006494/1, NE/H005927/1, NE/H007768/1, NE/H006540/1, NE/H005617/1). Simon Kemp, British Geological Survey (BGS), is thanked for undertaking the quantitative XRD analysis of the samples in this study. Michael Ward and Andy Brown, University of Leeds, are thanked for their help with conducting the TEM analysis. Gareth Law and Tim Marshall, The University of Manchester, are thanked for their help with the XANES data aquisition and Fred Mosselmans, Diamond Light Source, is thanked for his aid in the processing of the XANES data. Diamond Light Source are thanked for the access to beamline B18 (SP8544, SP8070 and SP7593) that contributed to the results presented here. A. E. Milodowski and C. Rochelle publish with the permission of the Executive Director of the British Geological Survey (NERC).

Appendix A. Supplementary material

Supplementary data associated with this article can be found, in the online version, at http://dx.doi.org/10.1016/j.apgeochem.2014.08.003.

References

Akbulut, A., Kadir, S., 2003. The geology and origin of sepiolite, palygorskite and saponite in Neogene lacustrine sediments of the Serinhisar-Acipayam Basin, Denzili, SW Turkey. Clays Clay Miner. 51, 279–292.

Alexander, R. (Ed), 1992. A natural analogue study of the Maqarin hyperalkaline groundwaters. I: Source term description and thermodynamic database testing. Nagra Technical Report NTB 91-10, Nagra, Wettingen, Switzerland.

Alexander, W.R., Dayal, R., Eagleson, K., Eikenberg, J., Hamilton, E., Linklater, C.M., McKinley, I.G., Tweed, C.J., 1992. A natural analogue of high pH cement pore waters from the Maqarin area of northern Jordan II: results of predictive geochemical calculations. J. Geochem. Explor. 46, l33–146.

Alexander, W.R., Milodowski, A.E. & Pitty A. F. 2011. Cyprus Natural Analogue Project (CNAP) phase III final report. Posiva Working Report WR 2011–77, Posiva, Eurajoki, Finland.

Alexander, W.R., Milodowski, A.E., Pitty, A.F., Hardie, S., Kemp, S.J., Korkeakoski, P., Rigas, M., Rushton, J.C., Sellin, P., Tweed, C.J., 2012. Reaction of bentonite in low-alkali cement leachates: an overview of the Cyprus Natural Analogue Project (CNAP). Mineral. Mag. 76, 3019–3022.

Andra, 2012. Low and intermediate level short-lived waste [online]. <http://www.andra.fr/international/pages/en/menu21/waste-management/waste-classification/short-lived-low–and-intermediate-level-waste-1609.html> (accessed 19/01/2014).

Atkins, M., Glasser, F.P., 1992. Application of Portland cement-based materials to radioactive waste immobilization. Waste Manage. 12, 105–131.

Atkinson, A., 1985. The time dependence of pH within a repository for radioactive waste disposal. UKAEA, AERE-R 11777.

Baes, C.F., Mesmer, R.S., 1976. The Hydrolysis of Cations. John Wiley & Sons, London.

Bateman, K., Coombs, P., Noy, D.J., Pearce, J.M., Wetton, P., Haworth, A., Linklater, C., 1999. Experimental simulation of the alkaline disturbed zone around a cementitious radioactive waste repository: numerical modelling and column experiments. Geological Society, London, Special Publications, 157, 183–194.

Berner, U.R., 1992. Evolution of pore water chemistry during degradation of cement in a radioactive waste repository environment. Waste Manage. 12, 201–219.

Berry, J.A., Baker, A.J., Bond K.A., Cowper, M.M., Jeffries, N.L., Linklater, C.M., 1999. The role of sorption onto rocks of the Borrowdale Volcanic Group in providing chemical containment for a potential repository at Sellafield. In: Metcalfe, R., Rochelle, C. (Eds.), Chemical Containment of Waste in the Geosphere. Geological Society of London, Special Publication. 157, 101–116.

Bérubé, M.-A., Choquette, M, Locat, J., 1990. Effects of lime on common soil and rock forming minerals. Appl. Clay Sci. 5, 145–163.

Birsoy, R., 2002. Formation of sepiolite-palygorskite and related minerals from solution. Clays Clay Miner. 50, 736–745.

Braithwaite, C.J.R., Heath, R.A., 2013. Alkali-carbonate reactions and 'dedolomitization' in concrete: silica, the elephant in the corner. Q. J. Eng. Geol.Hydrogeol. 46, 351–360.

Braney, M.C., Haworth, A., Jefferies, N.L., Smith, A.C., 1993. A study of the effects of an alkaline plume from a cementitious repository on geological materials. J. Contam. Hydrol. 13, 379–402.

Burns, P.C., Ewing, R.C., Hawthorne, F.C., 1997. The crystal chemistry of hexavalent uraniu: polyhedron geometries, bond-valence parameters, and polymerization of polyhedra. Can. Mineral. 35, 1551–1570.

Cuadros, J., Fiore, S., Huertas, F.J., 2010. Introduction to mixed-layer clay minerals. In: Fiore, S., Cuadros, J., Huertas, F.J., (Eds.), Interstratified clay minerals: origin, characterization and geochemical significance. AIPEA Education Series, Pub no.1. Digilabs, Bari, Italy.

Cuevas, J., 2004. Geochemical reactions in FEBEX bentonite. In: Michau, N. (Ed.), Ecoclay II: Effect of cement on clay barrier performance phase II. final report. European Commission. European contract FIKW-CT-2000-00018.

Derkowski, A., Bristow, T.F., Wampler, J.M., Środoń, J., Marynowski, L., Elliott, W.C., Chamberlain, C.P., 2013. Hydrothermal alteration of the Ediacaran Doushantuo Formation in the Yangtze Gorges area (South China). Geochim. Cosmochim. Acta 107, 279–298.

Eglinton, M., 2006. Resistance of concrete to destructive agencies. In: Hewlet, P.C. (Ed.), Lea's Chemistry of Cement and Concrete, fourth ed. Elsevier, pp. 843–863.

Fernandez, R., Rodríguez, M., Vigil De La Villa, R., Cuevas, J., 2010. Geochemical constraints on the stability of zeolites and C–S–H in the high pH reaction of bentonite. Geochim. Cosmochim. Acta 74, 890–906.

Fetter, C.W., 1999. Contaminant Hydrogeology, second ed. Prentice Hall, New Jersey, USA.

Gali, S., Ayora, C., Alfonso, P., Tauler, E., Labrador, M., 2001. Kinetics of dolomite–portlandite reaction: application to Portland cement concrete. Cem. Concr. Res. 31, 933–939.

Gaona, X., Kulik, D.A., Macé, N., Wieland, E., 2012. Aqueous-solid solution thermodynamic model of U(VI) uptake in C–S–H phases. Appl. Geochem. 27, 81–95.

Gaucher, E., Blanc, P., 2006. Cement/clay interactions – a review: experiments, natural analogues, and modeling. Waste Manage. 26, 776–788.

Glasser, F.P., 2001. Cement in radioactive waste disposal. Mineral. Mag. 65 (621), 633.

Grenthe, I., Drożdżyński, J., Fujino, K., Buck, E.C., Albrecht-Schmidtt, T.E., Wolf, S.F., 2008. Uranium. In: Morss, L.R., Edelstein, N.M., Fuger, J. (Eds.), The Chemistry of the Actinide and Transactinide Elements, third ed. Springer, Dordrecht, Netherlands.

Harfouche, M., Wieland, E., Dähn, R., Fujita, T., Tits, J., Kunz, D., Tsukamoto, 2006. EXAFS study of U(VI) uptake by calcium silicate hydrates. J. Colloid Interface Sci. 303, 195–204.

Hodgkinson, E.S., Hughes, C.R., 1999. The mineralogy and geochemistry of cement/rock reactions: high-resolution studies of experimental and analogue materials. Geological Society, London, Special Publications, 157, 195–211.

Hojati, S., Khademi, H., Cano, A.F., 2010. Palygorskite formation under the influence of saline and alkaline groundwater in central Iranian soils. Soil Sci. 175, 303–312.

Linklater, C.M. (Ed.), 1998. A natural analogue study of cement-buffered hyperalkaline groundwaters and their interaction with a repository host rock: Phase II. Nirex Science Report, S/98/003, UK Nirex Ltd., Harwell, UK.

Lorens, R.B., 1981. Sr, Cd, Mn and Co distribution coefficients in calcite as a function of calcite precipitation rate. Geochim. Cosmochim. Acta 45, 553–561.

Mäder, U., Fierz, T., Frieg, B., Eikenberg, J., Ruthi, M., Albinsson, Y., Mori, A., Ekberg, S., Stille, P., 2006. Interaction of hyperalkaline fluid with fractured rock: field and laboratory experiments of the HPF project (Grimsel Test Site, Switzerland). J. Geochem. Explor. 90, 68–94.

Milodowski, A.E., Hyslop, E.K., Pearce, J.M., Wetton P.D., Kemp, S.J., Longworth, G., Hodgkinson, E., Hughes, C.R., 1998. Mineralogy, petrology and geochemistry. In: Smellie, J.A.T. (Ed.), Maqarin Natural Analogue Study: Phase III. SKB Technical Report. (TR 98-04, Vols I and II). SKB, Stockholm, Sweden.

Min, D., Mingshu, T., 1993. Mechanism of dedolomitisation and expansion of dolomitic rocks. Cem. Concr. Res. 23, 1397–1408.

Nagra, 2014. Geological repository for low- and intermediate-level waste. <www.nagra.ch/en/tlsmae.htm> (accessed 19.01.2014).

NDA, 2010a. Geological disposal steps towards implementation. NDA report NDA/RWMD/013. NDA, Harwell.

NDA, 2010b. Geological disposal: near-field evolution status report. NDA/RWMD/033.

NDA, 2010c. Geological disposal radionuclide behaviour status report. NDA report NDA/RWMD/034. NDA, Harwell.

Nuclear Waste Management Organisation. 2010. DGR key features. <www.nwmo.ca/dgr_keyfeatures> (accessed 19.01.2014).

Parkhurst, D.L., Appelo, C.A.J., 2010. User's Guide to PHREEQC (Version 2)-A Computer Program for Speciation, Batch-Reaction, One-Dimensional Transport, and Inverse Geochemical Calculations, <http://web.inter.nl.net/users/pyriet/bijlage%206.pdf>.

Pfingsten, W., Paris, B., Soler, J., Mader, U., 2006. Tracer and reactive transport modelling of the interaction between high-pH fluid and fractured rock: Field and laboratory experiments. J. Geochem. Explor. 90, 95–113.

Pingitore, N.E., Eastman, M.P., 1986. The coprecipitation of Sr^{2+} with calcite at 25 °C and 1 atm. Geochim. Cosmochim. Acta 50, 2195–2203.

Poole, A.B., Sotiropoulos, P., 1980. Reactions between dolomitic aggregate and alkali pore fluids in concrete. Quart. J. Eng. Geol. Hydrogeol. 13, 281–287.
Ramirez, S., 2005. Alteration of the Callovo-Oxfordian clay from Meuse-Haute Marne underground laboratory (France) by alkaline solution. I. A XRD and CEC study. Appl. Geochem. 20, 89–99.
Ravel, B., Newville, M., 2005. ATHENA, ARTEMIS, HEPHAESTUS: data analysis for Xray absorption spectroscopy using IFEFFIT. J. Synchrotron Radiat. 12, 537–541.
Reardon, E.J., 1990. An ion interaction model for the determination of chemical equilibria in cement/water systems. Cem. Concr. Res. 20, 175–192.
Reardon, E.J., 1992. Problems and approaches to the prediction of the chemical composition in cement/water systems. Waste Manage. 12, 221–239.
Reynolds, R.C., Reynolds, R.C., 1996. Description of Newmod-for-Windows™. The calculation of one-dimensional X-ray diffraction patterns of mixed layered clay minerals. R.C. Reynolds Jr., 8 Brook Road, Hanover, NH.
Rochelle, C., Pearce, J., Bateman, K., Coombs, P., Wetton, P., 1997. The evaluation of chemical mass transfer in the disturbed zone of a deep geological disposal facility for radioactive waste: X. Interaction between synthetic cement porefluids and BVG: Observations from experiments of 4, 9 and 15 months duration. *BGS technical report* WE/97/16 Article permalink: <http://nerc.worldcat.org/oclc/703969750>.
Savage, D., Bateman, K., Hill, P., Hughes, C., Milowdowski, A., Pearce, J., Rae, M., Rochelle, C., 1992. Rate and mechanism of the reaction of silicates with cement pore fluids. Appl. Clay Sci. 7, 33–45.
Savage, D., Rochelle, C., 1993. Modelling reactions between cement pore fluids and rock: Implications for porosity change. J. Contam. Hydrol. 13, 365–378.
Savage, D., 2011. A review of analogues of alkaline alteration with regard to long-term barrier performance. Mineral. Mag. 75, 2401–2418.
Schlegel, M.L., Descostes, M., 2009. Uranium uptake by hectorite and montmorillonite: a solution chemistry and polarized EXAFS study. Environ. Sci. Technol. 43, 8593–8598.
Schwarzenbach, E.M., Lang, S.Q., Früh-Green, G.L., Lilley, M.D., Bernasconi, S.M., Méhay, S., 2013. Sources and cycling of carbon in continental, serpentinite-hosted alkaline springs in the Voltri Massif, Italy. Lithos 177, 226–244.
Sherman, D.M., Peacock, C.L., Hubbard, C.G., 2008. Surface complexation of U(VI) on goethite (α-FeOOH). Geochim. Cosmochim. Acta 72 (2), 298–310.
Soler, J.M., Mäder, U.K., 2007. Mineralogical alteration and associated permeability changes induced by a high-pH plume: modeling of a granite core infiltration experiment. Appl. Geochem. 22, 17–29.
Taylor, H.F.W., 1990. Cement Chemistry. Academic Press, London.
Techer, I., Bartier, D., Boulvais, P.H., Tinseau, E., Suchorski, K., Cabrera, J., Dauzères, A., 2012. Tracing interaction between natural argillites and hyper-alkaline fluids from engineered cement paste and concrete: chemical and isotopic monitoring of a 15-years old deep-disposal analogue. Appl. Geochem. 27, 1384–1402.
Tesoriero, A.J., Pankow, J.F., 1996. Solid solution partitioning of Sr^{2+}, Ba^{2+}, and Cd^{2+} to calcite. Geochim. Cosmochim. Acta 60, 1053–1063.
Tinseau, E., Bartier, D., Hassouta, L., Devol-Brown, I., Stammose, D., 2006. Mineralogical characterization of the Tournemire Argillite after in situ interaction with concretes. Waste Manage. 26, 789–800.
Tits, J., Geipel, G., Macé, N., Eilzer, M., Wieland, E., 2011. Determination of uranium(VI) sorbed species in calcium silicate hydrate phases: a laser-induced luminescence spectroscopy and batch sorption study. J. Colloid Interface Sci. 359, 248–256.
Xie, Q., Chen, T., Zhou, H., Xu, X., Xu, H., Ji, J., Lu, H., Balsam, W., 2013. Mechanism of palygorskite formation in the Red Clay Formation on the Chinese Loess Plateau, Northwest China. Geoderma 192, 39–49.
Yeniyol, M., 2007. Characterization of a Mg-rich and low-charge saponite from the Neogene lacustrine basin of Eskişehir, Turkey. Clay Miner. 42, 541–548.
Yeniyol, M., 2012. Geology and mineralogy of a sepiolite-palygorskite occurrence from SW Eskişehir (Turkey). Clay Miner. 47, 93–104.